Available online at www.sciencedirect.com
SCIENCE DIRECT®
Journal of Chromatography A, 1046 (2004) 175–184
JOURNAL OF CHROMATOGRAPHY A
www.elsevier.com/locate/chroma

Influence of ionic strength, sample size, and flow conditions on the retention behavior of pullulan in flow field-flow fractionation

Maria-Anna Benincasa*, Chiara Delle Fratte

Department of Chemistry VEC, University of Roma "La Sapienza", Ple A. Moro, 5, 00185 Rome, Italy

Received 11 February 2004; received in revised form 27 May 2004; accepted 15 June 2004

Abstract

Polymer molecular parameters such as hydrodynamic size are expected to be invariant regardless of the technique used to measure them, and to vary only, to some extent, with the solvent power and the polymer structure and properties as predicted from polymer chemistry. The hydrodynamic size of five pullulan standards derived from FlFFF in solutions of different ionic strength appears to correlate well to molecular mass as expected for neutral polymers for all fractions except that of lower mass. The correlation also holds for large amounts of injected sample even though with a slope which increases with rising polymer load. The evidence that the same result is obtained also for low sample amounts but with a higher cross-flow rate is interpreted as the manifestation of the presence of hydrodynamic interactions in concentrated polymer systems.

Keywords: Ionic strength; Sample size; Flow conditions; Retention behaviour; Flow field-flow fractionation; Field-flow fractionation; Overloading; Pullulan; Polysaccharides

1. Introduction

For their specific biosynthetic pathways polysaccharides, widely present in any living system, are generally found as broadly-disperse mixtures often heterogeneous in structure and composition. Besides vegetable and animal systems, several micro-organisms such as fungi, bacteria and algae, produce polysaccharides [1]. Of all microbial polysaccharides the pullulan synthesized by the polymorphic fungus *Aureobasidium pullulans* is probably the most studied. The role of this polysaccharide in the cycle of *A. pullulans* has not been unequivocally elucidated and some authors favour its function as a cell wall component while others support its action as a protecting agent from harsh environmental conditions [2]. Unlike the most common β-linked microbial polysaccharides, the neutral pullulan appears to be a linear α-glucan of maltotriose units, possibly with occasional branching of glucosyl or maltosyl substitution which, however, does not affect its solution behavior which appears to be that of a flexible, statistical coil. Unless produced under carefully controlled fermentation conditions, pullulan shows considerable variability in molecular mass (*M*). It appears that molecular mass (and in general the yield and composition of microbial exopolysaccharides) strictly depends on the fungal strain as well as on the incubation conditions [3]. Growth time in particular, is reported to affect molecular mass which seems to decrease with increase in incubation time, probably due to cleavage of the polysaccharide chain by an extracellular amylolytic enzyme.

Even though dextran is often used as a standard for polymer analysis, pullulan, commercially available as fractions of narrower distribution and in a broad molecular mass range, generally exhibits more symmetric distributions and is a preferred standard polymer in aqueous solutions. Here, pullulan has been employed as a test material to study the elution behavior of neutral water-soluble polymers in flow field-flow fractionation (flow FFF).

* Corresponding author. Tel.: +39 (0)349 3423344; fax: +39 06 490631
E-mail address: mariaanna.benincasa@uniroma1.it (M.-A. Benincasa).

0021-9673/$ – see front matter © 2004 Elsevier B.V. All rights reserved.
doi:10.1016/j.chroma.2004.06.092

FFF, a flow-assisted analytical technique is clustered in the same category of separations as chromatography for the particular combination of the flow structure and field, similar to that found in that methodology [4]. Much like more frequently used chromatographic techniques the transport flow carrying species along the separation chamber is continuous and orthogonal to the externally applied field. The latter, interacting with some component-specific property, induces compression of the sample particles (or molecules) on one of the channel wall denominated the accumulation wall. The thickness of the zone results from the combined effect of the compressing field and the dispersing action of diffusion. It is demonstrated that the outcome of these phenomena is a steady-state concentration distribution of molecules exponential in nature, highest at the accumulation wall and decreasing away from it, toward the center of the channel [5].

The position of the migrating sample cloud is identified by the exponential constant ℓ given by the ratio $\Re T/F$ with $\Re$ being the Boltzmann constant, T the absolute temperature and F the force exerted by the field. For its dependence on the ratio of energy and force, which gives ℓ the dimension of length, this parameter is viewed as the zone mean elevation above the accumulation wall. In the parabolic distribution of the transport fluid velocities, higher elevation of the sample envelope translates into a higher migrating velocity. For convenience the ℓ value scaled to the channel thickness w is most commonly used in the equations. The dimensionless parameter $\lambda = \ell/w$ in flow FFF may be obtained from Eq. (1):

$$\lambda = D\frac{V^0}{w^2}\frac{1}{\dot{V}_c} \tag{1}$$

Considering that V^0 and w^2 are channel geometrical parameters, therefore instrumental constants, λ in FlFFF only depends on the particle diffusion coefficient D and cross-flow rate $\dot{V}_c$. If the latter also is kept constant the only parameter determining the value of λ is the specific molecular diffusivity. Stokes and Einstein studies showed that at zero concentration the diffusion coefficient D_0 is related to the particle radius R_0 as:

$$D_0 = \frac{\Re T}{6\pi\eta R_0} \tag{2}$$

R_0 is unambiguously determined only for rigid spherical particles (at molecular level well represented by globular proteins) and may vary for polymers in solution to a different extent depending on the system properties. For flexible chain macromolecules in particular, molecular size is defined as the average of all possible conformations of same free energy and varies with the calibre of intra-particle interactions relative to the interactions between the polymer and solvent. At constant temperature T the solvent power is, therefore, the primary factor affecting the molecular size of random coil polymers in infinitely dilute solutions. Physical-chemistry of macromolecules indicates a power correlation between R_0, hence D_0, and the molecular mass of flexible chain polymers expressed as [6].

$$D_0 = AM^{-b} \tag{3}$$

In Eq. (3) the coil compactness is expressed by the b-exponent predicted to be around 0.5 for ideal systems at Θ-conditions and increasing in the presence of strong interactions between the polymer and the solvent that would lead to molecular enlargement. Combination of Eqs. (1) and (3) gives:

$$\lambda = AM^{-b}\frac{V^0}{w^2}\frac{1}{\dot{V}_c} \tag{4}$$

Eq. (4) appears to be valid under any experimental condition. However, since the rigorous mathematical treatment of the partitioning mechanism in FFF considers rigid particles without volume and mass, it is assumed that no volume is forbidden to the particle displacement under the diffusive or convective action. The ideal situation would then occur when dilution of the migrating zone were infinite. While, in practice, this can not be achieved, it is possible to adjust the working parameters to minimize non-ideal effects. This may be obtained for instance by both injecting the smallest possible amount of sample and/or reducing compression by the field. Both these procedures by allowing the sample to distribute into a larger volume would enhance dilution. The plug extension along the migration axis z (arising from the longitudinal diffusion in the presence of differences in concentration along the channel) also contributes to increase the zone volume. A number of other factors contribute to modify this volume from that initially injected (V_{inj}). Among these the hydrodynamic dispersion due to the non-uniform flow profile across the channel is recognized as the dominant factor in zone broadening [7]. The overall breadth of the zone is given by summing the variances of all the independent processes occurring during elution. Even though a number of factors (particle longitudinal diffusion, sample distribution across the channel before relaxation [8], finite volume of the injected sample plug [9], unequal particle velocity due to the non-uniform flow profile and different elution rates of species with different molecular size in polydisperse samples [10]) by independently contributing to this value should be added up to get the total variance [11], the latter results to be well represented also simply as:

$$\sigma^2 = \sigma^2_{inj} + \sigma^2_{neq} + \sigma^2_{poly} \tag{5}$$

since the influence of the first two processes may become negligibly small under specific operating conditions (higher eluent velocity and relaxation procedure). The first term in Eq. (5) may be calculated:

$$\sigma^2_{inj} = \frac{1}{12}\left\langle\frac{V_{inj}L}{V^0}\right\rangle^2 \tag{6}$$

It is seen that σ^2_{inj} in Eq. (6) only depends on the volume of the injected sample since the length L and volume V^0 are constant for a given channel. This term may therefore be

minimized and made constant if the same low sample volume V_{inj} is injected. This procedure however has the drawback of limiting the injected mass or increasing the initial sample concentration. σ^2_{neq} and σ^2_{poly} are the terms more strongly affecting band spreading, the first one for its dependence on the carrier mean velocity and sample diffusivity, the second for the contribution to zone enlargement by differences in the polymer size and mass (M) i.e. polydispersity μ.

Zone width (hence the factors affecting it) is considered here for its role in determining the sample bi-dimensional concentration during elution [12].

$$c(x, z) = c_{00} \exp\left\langle \frac{-(z - Z)^2}{2\sigma^2} \right\rangle \exp\left\langle \frac{-x}{\lambda w} \right\rangle \quad (7)$$

In Eq. (7) z is the longitudinal axis and x the distance across the channel. c_{00}, the highest concentration attained at the accumulation wall in the center of the Gaussian distribution is found from:

$$c_{00} \cong \frac{V_{inj} c_{inj} L}{\sqrt{2\pi\sigma^2} V^0 \lambda} \quad (8)$$

where c_{inj} is the concentration of the sample solution before injection. Eq. (8) shows that c_{00} may largely exceed the polymer initial concentration since λ is always lower than unity and decreases as retention increases. The maximum concentration c_0 however is achieved at the accumulation wall before elution begins, i.e. when under the effect of the field alone the sample is exponentially distributed across the channel thickness. Under this condition $c_0 \sim c_{inj}/\lambda$ and a remarkable magnification of the initial concentration is registered.

From the above equations, it appears that the volume and concentration of the injected sample would change the zone concentration but would not directly affect retention. Under linear conditions we should then expect only a different detector response as V_{inj} and c_{inj} increase but no change in retention parameters. If, in the presence of the so-called overloading phenomena retention is affected, and if we assume that all the above equations still apply under these conditions then it should also be assumed that the increased concentration influences the only parameter responsible of the retention level i.e. in flow FFF, the particle diffusive motion. The overall molecular displacement occurring under these conditions, which has been termed "apparent diffusivity" and is treated through an apparent diffusion coefficient D_{app}, would then represent the outcome of multiple mechanisms but the simple thermal energy-induced motion of isolated particles in an undisturbed medium.

Of the different concentration regimes recognized in polymer chemistry for macromolecules in solution only the dilute regime is governed by properties of individual macromolecules. Since the threshold regime between the dilute and semidilute (or concentrated) solution is determined by the concentration where coils just touch each other the critical concentration c^* is of the same order of magnitude as that of the monomers in each coil. This concentration is obtained as the ratio of the number N of the effective segments in a polymer chain to the volume V of each coil. Since for an ideal chain the latter depends on N as a 3/2 power c^* results to be proportional to $N^{-1/2}$. This translates into a sharp decrease of the polymer critical concentration as N increases. Consideration of the excluded volume for self-avoiding chains gives a power dependence of c^* as $N^{-4/5}$ and consequently with the same rate on molecular weight. Since in a polymer chain $N \gg 1$ the threshold density for the critical concentration is fairly small. Concentration may influence macromolecules' dynamics well before c^* is reached. The diffusivity (as well as other parameters such as viscosity) of polymers in solutions of increasing concentration has been widely studied [13–16] to determine molecular parameters such as chain flexibility [13].

The concentration driven co-operative mechanism (thermodynamic force) contributing to determine the band thickness in flow FFF, would tend to enhance diffusivity as concentration increases. On the other hand, however, in the absence of other effects such as electrostatic interactions, the coil mobility is expected to decrease as concentration rises because the hydrodynamic perturbations on the surrounding medium deriving from the presence of other macromolecules may retard the diffusive motion (hydrodynamic interactions) [15,16]. Hence various correlations are found for the effect of concentration on D of polymers depending on the diffusive mechanism investigated, the properties of the polymer solution, the concentration range and sample molecular mass.

In this work, we report the study of the influence of sample volume and concentration on the retention of the neutral pullulan carried out in solutions of different ionic strength on five polymer fractions of varying molecular mass.

2. Experimental

The retention behavior of the pullulan standards P10, P50, P100, P200 and P400 (Showa Denko K.K., Tokyo, J), was studied in a flow FFF system from Postnova Analytics (Salt Lake City, UT, USA). The channel obtained from a sheet of mylar had a length L of 29.75 cm, a breadth b of 2.0 cm, and a thickness w of 0.0254 cm. The PLBC membrane of regenerated cellulose from Millipore (Bedford, MA, USA) had a molecular weight cut-off of 3 kDa. The two HPLC pumps used to drive the channel and field substreams were respectively a Shimadzu LC-9A (Kyoto, Japan) and Perkin-Elmer Series 2 (Norwalk, CT, US). The system set-up comprised also a variable back-pressure regulator (Alltech Associates, Deerfield, IL, USA) on the channel line and a constant pressure regulator (Upchurch, Oak Harbor, WA, USA) setting the back-pressure of the cross-flow. Sample injection was performed through a silicon septum placed in a tee-union to avoid limitations in the injected volume. Sample solutions, whose concentration is specified in the text for each experiment, were also filtered through a 0.45 μm zero dead volume

filter placed after the injection port. The concentration profile of the eluting band obtained by a differential refractive index detector RID 10-A from Shimadzu was recorded on computer by in-house software package. Distilled water, deionized and filtered through an ion-exchanger/ultrafiltration device from USF (Ransbach-Baumbach, D) and aqueous salt solutions of Na_2SO_4 (Carlo Erba, Mi, IT) served as carriers. All the data were processed using the temperature measured during the experiments.

3. Discussion

The elution profiles of five narrowly-disperse fractions of pullulan standards with molecular masses of 12,200, 48,000, 100,000, 186,000 and 380,000 Da shown in Fig. 1 were acquired by injecting 3 μg of each sample, except for the 380,000 Da fraction, for which 5.5 μg were used. All samples were dissolved in water which also served as the carrier liquid. The good reproducibility of the elution curves is manifested by the invariant size distribution of three runs of the 186,000 Da fraction displayed in the inset of the same figure. The size distribution, rather than the time-based fractogram, is plotted since molecular dimension is the physico-chemical parameter expected to be invariant even if differences in the flow conditions were registered, the latter being accounted for during conversion of the elution curve to size distribution.

Diffusion data widely available in polymer literature may be obtained using diverse analytical techniques. In some case however, because of the limited range of applicability of each technique, different methods are utilized for different *M* fractions of the same polymer [17]. This procedure is followed even though diverse methodologies respond to different diffusive mechanisms, as in the case of the boundary formation acting in a concentration gradient, and photon correlation spectroscopy (PCS) where differences in concentration are ruled out a priori. It is, therefore, not surprising that values of the diffusion coefficient reported for the pullulan in Table 1 differ as much as 30%, with this discrepancy varying with molecular mass. The values of D_{app} reported for the five pullulan standards have been determined as the average of 5–10 independent FlFFF runs of 3.0 μg injection load for each polymer fraction under experimental conditions identical to those of Fig. 1. To allow a consistent treatment of the experimental curves the data and standard deviations were evaluated at the retention time corresponding to the first moment of the gaussian best fit of the eluted peak. This procedure has been applied throughout this work even though, due to the high symmetry of the pullulan peaks, differences between the t_r determined in this way and that calculated at the response maximum were negligible. Inspection of Table 1 shows that the values of D_{app} derived from flow FFF are closer to those obtained using the free boundary formation method in the same aqueous medium [18]. This result is not surprising if it is considered that in both methods the diffusive mechanism acts in a concentration gradient.

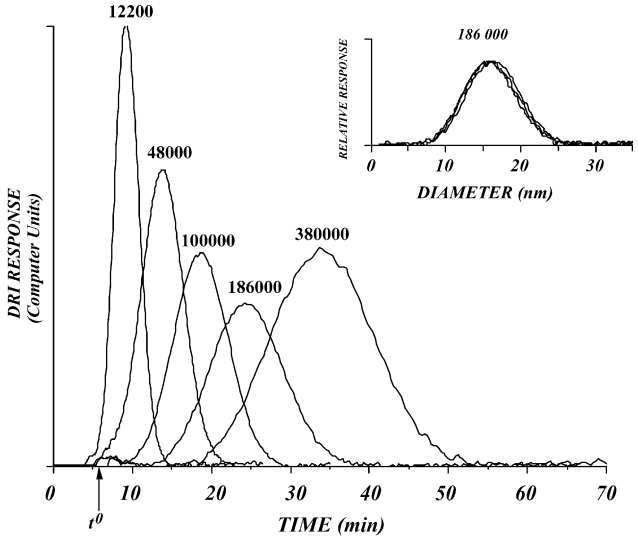

Fig. 1. FlFFF fractogram of five pullulan standards of the nominal molecular mass shown. Injected sample concentration was always 1 mg/mL. $\dot{V} = 0.2$ mL/min and $\dot{V}_c = 0.6$ mL/min with the water eluent. Differential refractive index detection. In the inset: size distribution obtained from repeated elutions of 3 μg of the pullulan 186,000 Da.

Table 1
Pullulan diffusion coefficients D^0 ($\times 10^{-7}$ cm^2 s^{-1})

	Water[a]	Water[b]	0.02% NaN_3[c]	0.2% NaN_3[d]
P10	11.44 ± 0.56	10.5	9.56	
P50	5.57 ± 0.12	4.2	3.45	
P100	3.88 ± 0.05	3.5	2.93	2.56
P200	2.65 ± 0.05	2.35	2.21	1.94
P400	1.80 ± 0.05	1.60	1.40	1.34

The temperature for the FlFFF experiments was always 20 °C.
[a] Diffusion coefficient and standard deviations obtained from flow FFF.
[b] Data from reference [18], obtained by the boundary formation method.
[c] Data from reference [17], obtained by PCS for the P50–400 samples and free diffusion for the P10.
[d] Data from reference [23], obtained by DLS.

The power law expressed by Eq. (3) relating the diffusion coefficient to the polymer molecular mass, manifests the macromolecules' conformation through the value of the *b* exponent, which may be obtained from the slope of the linear correlation between the logarithm of parameter *D* and *M*. For the pullulan this correlation, and the corresponding regression coefficient, obtained from the retention parameters of 3 μg of each polymer (Eq. (1)) is seen to change depending on whether the 12,200 Da fraction is considered (Fig. 2b) or not (a). The value of 0.546 for the slope obtained in water for the four higher *M* polymers, which is in good agreement with independent data [18] decreases to 0.537 if the 12,200 Da fraction is included in the calculations. The even lower value of 0.535 obtained considering only the two lower *M* polymers (12,000 and 48,000) would suggest a different conformation of the shorter chain pullulans. This speculation, in agreement with results reported by

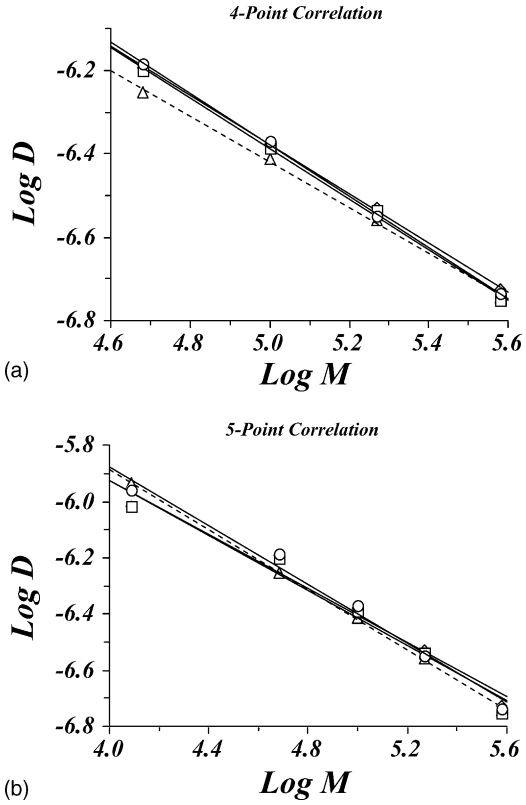

Fig. 2. Log–log plots of apparent diffusion coefficient vs. molecular mass obtained at different ionic strength for the pullulan 48,000, 100,000, 186,000 and 380,000 Da (a). (b) Five-point log–log correlation including the value for the 12,000 Da fraction. △ = water, ◊ = 7.7 mM, □ = 15 mM, ◯ = 75 mM ionic strength of the Na_2SO_4 aqueous solution.

other authors [17,18] is confirmed by investigation in solutions of 7.7, 15 and 75 mM ionic strength where the difference in the *b*-value when the 12 kDa polymer is considered is even more remarkable. In particular, the *b*-exponent gradually increases the many more higher *M* standards are included in the correlation. Consideration of the two lower *M* polymers only, for the log *D*–log *M* plot decreases the slope to less than 0.4. Accordingly, the 5-point correlation coefficient R^2 worsens remarkably compared to that given by the 4-point fit and goes from 0.9990 to 0.97. Several mechanisms may be claimed to explain the behavior of the lower *M* pullulan particularly considering that the greater departure of the diffusion coefficient data appears in solutions of higher *I* than water. Polymer-ion interactions specific only to polymer fractions of lower dimensions are known for other polymers [19 and references therein] and would well apply to this polymer. However, a more complex molecular architecture for this polysaccharide than that of a regularly linear, flexible homopolymer in the whole molecular weight range may be also taken into account [18] and may better support the previous hypothesis. Altogether these results convey the idea that more extensive investigations would be needed to definitely shed light on the composition and behavior of the pullulan polysaccharide.

3.1. Influence of the injected mass and solvent ionic strength

As argued in the introduction the sample concentration c_{inj} and volume V_{inj} determining the effective concentration and width of the eluting band, Eqs. (7) and (8), are not expected to affect retention as long as the system follows an ideal behavior. The profiles of the pullulan 48,000, 100,000 and 380,000 Da registered in water for increasing injected volumes at the constant c_{inj} of 5 mg/mL, illustrated in Fig. 3a, contradict this expectation. The increase in retention time with injected volume (i.e. mass) is clearly more pronounced for the higher molecular mass polymer fractions. Indeed, while the lowest *M* compound shows a slight change in the peak maximum t_r only for the 200 μg load, the same effect on the 380,000 Da polymer appears already with 45 μg injection. Larger loads of this sample involve an overall peak shift to higher t_r and evident band broadening. The use of an electrolyte solution of 75 mM ionic strength does not suppress all influence of sample mass on retention as shown in Fig. 3b even though it reduces peak shifts for all the fractions and more substantially for the 380,000 Da polymer. A more quantitative picture of these results is obtained by plotting the hydrodynamic diameter of the three standards of Fig. 3a and b as a function of the injected mass. d_h in Fig. 4 was evaluated following the same procedure described for the data of Fig. 2 and using Eq. (2), for both the water carrier and the aqueous solution of Na_2SO_4 of 75 mM ionic strength. For the calculations the measured temperature and corresponding solvent viscosity were always used. As evident in Fig. 4 the presence of the electrolyte brings about an overall reduction of the measured molecular dimensions which is more substantial for the larger *M* polymer whose higher chain flexibility allows the coil to respond more remarkably to the lower solvating power of the salt solution. In any case the conspicuous response of the 380,000 Da polymer to increasing m_{inj} is the clearest indication of the trend of increasing measured molecular size with sample load common to all the polymer fractions as shown in Fig. 3a and b. These results call for further discussion. The effect of the injected mass displayed in these figures cannot be considered typical for any polymer system. It has been shown that the behavior of charged polymers in concentrated solutions at low ionic strength is opposite of that seen here with retention decreasing as the amount injected is raised [19,20]. Therefore, in the case of polyelectrolytes, *D*-values increase accordingly [21]. Contrariwise the FFF retention level of neutral polymers is consistently seen to increase with sample load regardless of the type of field employed [12,22]. This inference is confirmed here by the behavior of the pullulan in aqueous FFF, a sample system which only shares with previous systems [12,22] the neutral nature of the polymer.

The least-square best fits for the data of Fig. 4, reported in Table 2, allow extrapolation of d_h at zero concentration. These values listed in Table 3 together with the dimensions obtained from the low load experiments of Fig. 1 show that

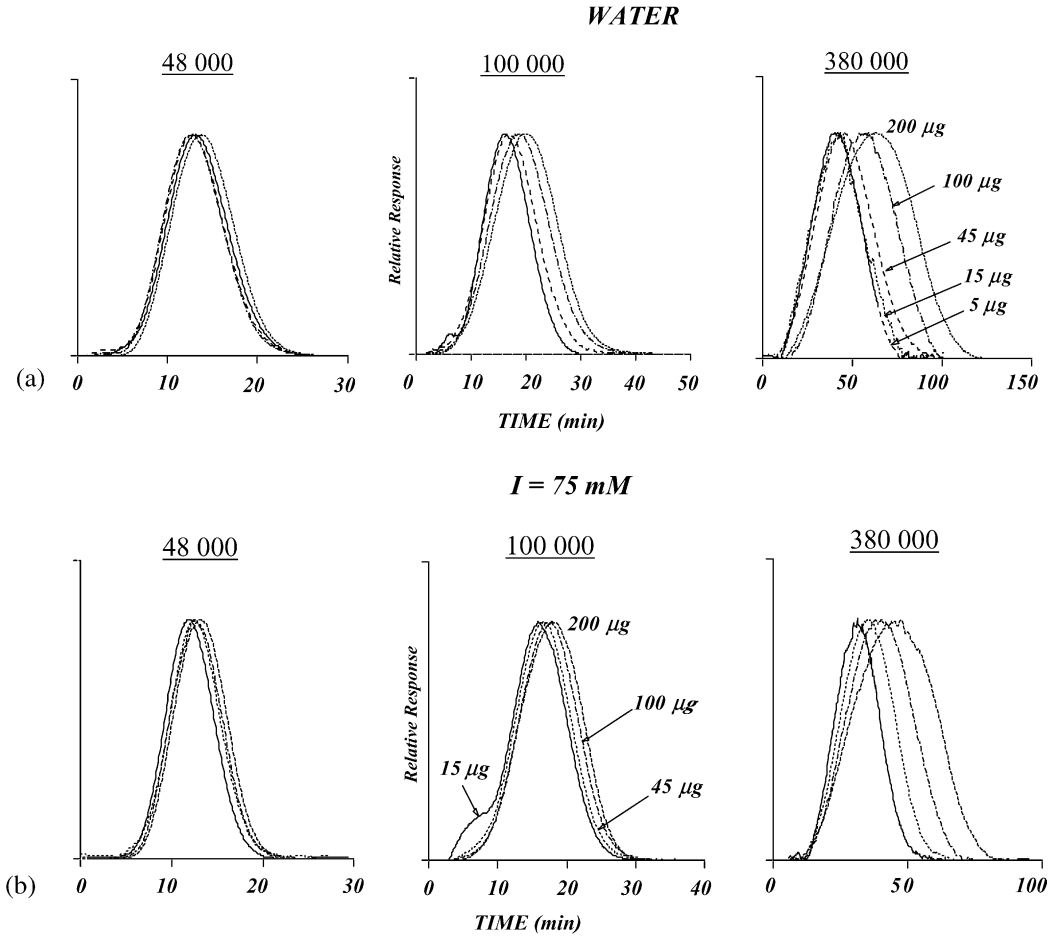

Fig. 3. (a) Retention profiles of pullulan 48,000, 100,000 and 380,000 Da obtained in water at increasing injected sample volume. c_{inj} = 5 mg/mL in all experiments. Flow conditions and detection as in Fig. 1. (b) Fractogram of the same pullulan fractions of part (a) registered in aqueous Na_2SO_4 of I = 75 mM. Same line style corresponds to the same injected amount.

the latter differ by 5–9% in water from those numerically extrapolated to infinite dilution. In particular measured and extrapolated d_h are comparable in both eluents for the lower M fractions but differ rather remarkably for the 380,000 Da standard in water. This observation further support the evidence of Figs. 3 and 4 that the influence of the sample injected mass depends on the polymer characteristics as well as on the solvent properties. The stronger interactions between macromolecules and a good solvent in general do not facilitate polymer analysis [12,19,20,21].

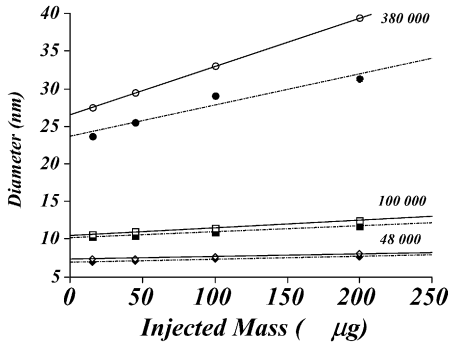

Fig. 4. Hydrodynamic diameter measured by flow FFF for the pullulans 48,000, 100,000 and 380,000 Da plotted versus injected load. Carrier liquids were water (open circles) and a Na_2SO_4 solution of I = 75 mM (solid circles). c_{inj} = 5 mg/mL throughout.

Table 2
Correlations between measured hydrodynamic diameter (d_h) and injected mass (m_{inj}) obtained in aqueous solutions of different ionic strength

Sample	Water	Ionic strength 75 mM
P50	$d_h = 7.29 + 0.00376 m_{inj}$	$d_h = 6.92 + 0.00405 m_{inj}$
P100	$d_h = 10.53 + 0.00994 m_{inj}$	$d_h = 10.21 + 0.00790 m_{inj}$
P400	$d_h = 26.46 + 0.08931 m_{inj}$	$d_h = 23.71 + 0.04119 m_{inj}$

Table 3
d_h (nm) measured for 3 µg of sample at c_{inj} = 1 mg/mL and values extrapolated to zero mass from the plots of Fig. 4

Sample	Water		Ionic strength 75 mM	
	3 µg	Extrapolated	3 µg	Extrapolated
P50	7.7	7.3	7.3	6.9
P100	11.1	10.5	10.9	10.2
P400	23.8	26.5	23.6	23.7

Because of the linear dependence of the diffusion coefficient on molecular dimensions (Eq. (2)), when correlated to molecular mass the logarithm of d_h for a polymer at zero concentration is expected to fit a linear function with the same slope of the log D–log M plot:

$$\log d_h = \log A' + b' \log M \quad (9)$$

The same correlation is not necessarily expected for concentrated solutions unless it is assumed that a scaling mechanism still acts under conditions where the particle motion might be affected by various interactions between particles or with a perturbed surrounding medium. In this case it should then, also be assumed that these interactions have a scaling pattern. The linear data reductions obtained from experiments at increasing polymer load in Fig. 5a and b fit very well the experimental values as confirmed by the correlation coefficients reported in Tables 4 and 5. Further inspection of these results shows that the slope of the plots rises as the injected amount increases which ironically implies that the separation selectivity improves the farther the conditions are from ideality. These experimental evidences deserve a more detailed analysis. The increasing values of the b-exponent for more consistent sample amounts can not be interpreted in this case according to polymer theory as indicative of molecular elongation [6] since no mechanism would justify coil expansion in more concentrated solutions. Nevertheless, the good correlation between molecular dimensions and mass reveals that molecular hydrodynamics still follows a scaling pattern in concentrated solutions of pullulan. This rules out the presence of aggregation which is generally a random process. Further support to the absence of aggregation is offered by the evidence that, as theoretically predicted, molecular size decreases when the pullulan is in electrolyte solutions (solid symbols in Fig. 4) rather than in water (open symbols in Fig. 4). To the contrary, aggregation which produces particles of larger size is generally emphasized in higher ionic strength solutions. It is also noted that the increase of the b-value for larger sample loads is more limited in salt solutions and the value obtained from the 3 μg load with a dilute sample solution more closely approaches that found by extrapolation to zero sample mass.

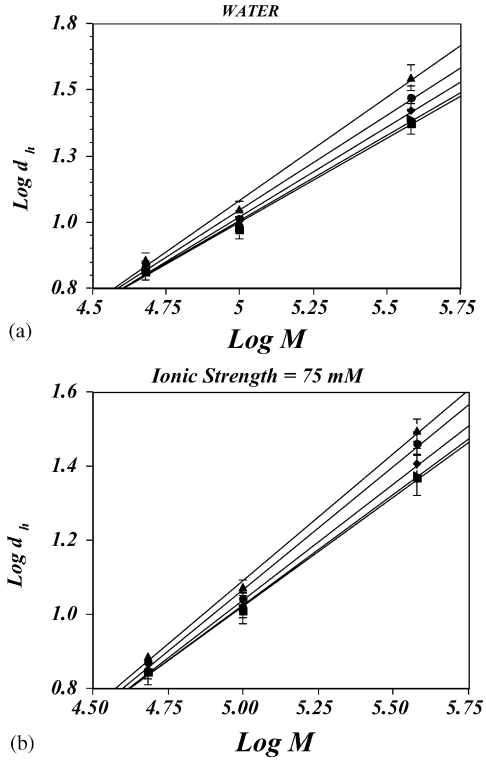

Fig. 5. Logarithm of the hydrodynamic diameter of pullulan measured in water (a) and at 75 mM ionic strength (b) correlated to the logarithm of molecular weight. The corresponding equations are reported in Tables 4 and 5. The plots from (a) to (b) in each diagram refer to injected amounts of 200, 100, 45 and 15 μg, respectively. The lowest plots (square symbol) are obtained by extrapolation to zero concentration.

Table 4
Correlation of the logarithms of d_h and M for pullulan obtained from FlFF in water

Injected mass (μg)	Log d_h	r^2
200	0.780 log M–2.768	0.993
100	0.714 log M–2.475	0.992
45	0.677 log M–2.316	0.994
15	0.644 log M–2.164	0.993
Extrapolated to zero	0.633 log M–2.114	0.994

Sample concentration = 5 mg/mL.

From these results it would appear that sample concentration is reflected into the terms log A' and b' of Eq. (9) as additive contributions to the correspondent values at infinite dilution. The log A' term valid at any polymer concentration is, therefore, broken down as log A + log α with the former referring to ideal solutions and the latter accounting for contributions other than those considered in theory. By similar considerations the b' exponent is equaled to $b + \Phi$ with b the value at zero concentration. Eq. (9) made explicit for A' and b' becomes:

$$\log d_h = \log A + b \log M + \log \alpha + \Phi \log M \quad (10)$$

where log A + b log M would account for the molecule's undisturbed dimensions and the log α + Φ log M would give an estimate of contributions due to concentration. These contributions in the present study are quantified by the b' and log A' plots versus the amount of injected sample. The correlations obtained are $b' = 0.63691 + 7.318 \times 10^{-4}\, m_{inj}$ in water and

Table 5
Log d_h–log M correlation for pullulan from flowFFF in 75 mM ionic strength solution

Injected mass (μg)	Log d_h	r^2
200	0.687 log M–2.341	0.997
100	0.667 log M–2.268	0.994
45	0.625 log M–2.088	0.997
15	0.596 log M–1.956	0.999
Extrapolated to zero	0.590 log M–1.925	0.998

Sample concentration = 5 mg/mL.

b' = 0.59593 + 5.0786 × 10^{-4} m_{inj} at I = 75 mM; $\log A'$ = −2.1336 − 0.00325 m_{inj} in water and $\log A'$ = −1.9573 − 0.002168 m_{inj} at 75 mM ionic strength. Considering that the coefficients R^2 for the b' plots were 0.9924 in water and 0.91469 in salt solution and for the $\log A'$ 0.9909 in water and 0.8976 at 75 mM ionic strength higher order terms have not been considered. In the b' expression the coefficient of the variable m_{inj} would represent the value of Φ in Eq. (10) per unit mass increase whereas the coefficient in the $\log A'$ expression would be the gradient of $\log \alpha$ per unit mass. The above treatment should only be considered a phenomenological approach since any rigorous investigation should refer to the polymer concentration rather than mass. Such a treatment is complicated in FFF by the continuous change of concentration during elution and the strong gradients in the same zone as shown in Eq. (7). It is, however, worth noting that scaling laws are still followed for the elution of large amounts of analyzed polymer (Fig. 5) which implies a non-random effect of the sample mass on the measured hydrodynamic parameters. Our interpretation is that these results reflect the effect of hydrodynamic interactions i.e. the perturbation on one particle motion by the flow field created by a nearby particle's movement in the same liquid medium. These interactions predicted to retard macromolecules' motion as concentration increases were shown to follow a scaling model [15,16]. On these assumptions the value of b lower in electrolyte solution than in water (Tables 4 and 5) may be considered as the manifestation of the decreased solvating power of the medium on the macromolecules as it is expected from the general scaling theory of polymer chemistry.

3.2. Effect of the flow conditions

Eqs. (1) and (4) show that the level of retention in FlFFF is solely determined by the field intensity and particle characteristics. The latter for the same macromolecule are expected to be invariant if measured under different flow conditions. The hydrodynamic parameters of the 48,000, 100,000 and 186,000 Da pullulans, their correlation to M and sample recovery have been studied in experiments differing from that of Fig. 1 only for the field intensity. As illustrated in Fig. 6 the elution profiles of these polymers obtained with $\dot{V}_c$ = 1.2 mL/min appear to have the expected symmetric profile well reproducing the theoretical Gaussian function as determined by computer fit. Lack of peak distortion hence would suggest the absence of non-ideal secondary effects. Nevertheless, the measured hydrodynamic sizes, shown in the same Fig. 6, differ by 13–35% from those measured for the same fractions at half cross-flow rate and reported in Table 3. The hydrodynamic diameter of the 186,000 Da pullulan, not shown there, was 16.2 nm. Sample interactions with the membrane are often claimed to be responsible of similar behavior. Such phenomena however, expected to yield incomplete sample recovery and possibly to lead to peak distortion, should also break the correlation between retention parameters and molecular mass since elution, i.e. t_r, would depend on the extent and number of such interactions. By contrast, the 100% absolute recovery [24] obtained for these pullulans and the correlation found between molecular parameters and molecular mass are not consistent with a mechanism involving random interactions of the sample polymer with the membrane material. As a matter of fact the logarithmic plots and the corresponding functions in Fig. 7 show that the flow FFF extrapolated hydrodynamic size of the three pullulans of Fig. 6 is still well correlated to the polymer molecular mass when a higher cross-flow rate is used. However, in this case the slope increases in a similar fashion to that obtained with large amounts of injected sample (Fig. 5). Considering that a higher field intensity reduces the sample envelope thus increasing the effective concentration during elution, the higher b-value obtained at $\dot{V}_c$ = 1.2 mL/min simply reflects the higher sample concentration much in the same way as it manifested larger m_{inj} as seen in Fig. 5. This is a logical interpretation of the consistent behavior shown by the pullulan anytime a

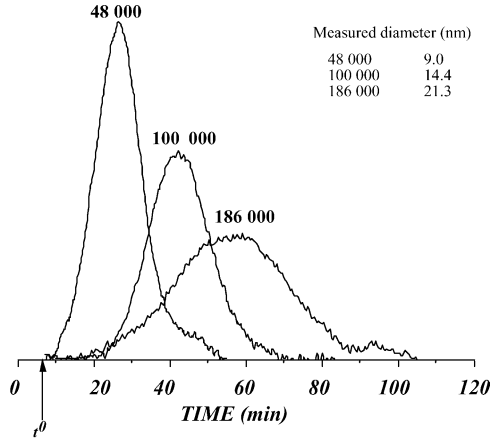

Fig. 6. Elution profiles of 3 μg of the pullulan standards shown in the labels. All the conditions as in Fig. 1 except for $\dot{V}_c$ = 1.2 mL/min. The d_h measured for each polymer is reported in the inset.

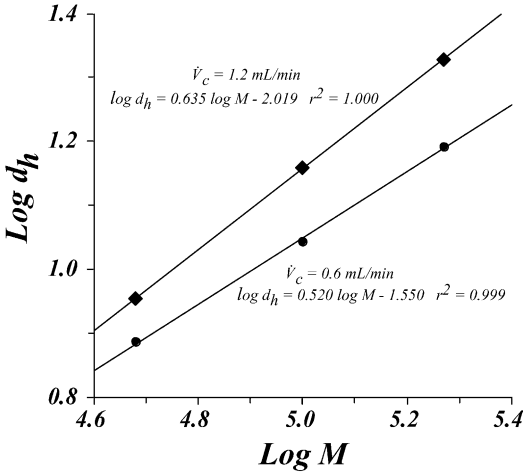

Fig. 7. Log d_h–log M plots for three pullulans obtained varying the cross-flow rate. $\dot{V}$ = 0.2 mL/min in all experiments with the water eluent. DRI for 3 μg injection of each polymer.

change in the experimental conditions led to a raise of the effective concentration of the eluting sample.

It would look from all the above results that using larger sample loads would only offer the advantage of enhanced detector response, thus reduced signal-to-noise ratio, and better separation selectivity. However the increased retention time may result in a big penalty in the analysis of high M samples that would elute in broader zones and with unacceptably long elution times. In this instance the increased band width would limit the detection enhancement given by the higher m_{inj}. In addition to this the sample parameters obtained under such conditions would not correctly reveal the polymer nature and properties.

4. Conclusions

Even though retention in FFF may be affected by a number of experimental parameters, under carefully tuned work conditions neutral polymers in aqueous flow FFF show a behavior very close to that of ideal systems. Such a conclusion is based on measurements of the apparent diffusivity of five pullulan standards extrapolated from low-load flow FFF which result to be well in agreement with reported data obtained by other techniques. Not surprisingly the agreement appears to be particularly good with results from the free diffusion method which, unlike other methods, acts under a concentration gradient, a condition similar to that experienced by molecules in FFF. When low sample concentration is used, even small departures from the theoretically predicted correlation between sample parameters may not be meaningless but rather stemming from effective differences in the sample properties. By contrast, when experimental conditions that enhance the zone concentration are used, molecular parameters measured from FlFFF do not remain invariant as predicted from FFF theory and would be expected from polymer chemistry. Their change however for the pullulan polysaccharide does not appear to be random or uncorrelated to the sample properties. The theoretically predicted relationship between the diffusivity derived equivalent size and molecular mass is still followed, even though with correlation constants increasing as the amount of sample increases. These results can not be explained on the basis of random mechanisms of molecular aggregation or polymer–membrane interactions. The interpretation based on the hydrodynamic interaction model predicting a retardation of a molecule's free diffusing movement with increased concentration seems to better explains the data of pullulan consistently scaled to molecular mass for all the sample loads investigated.

Nomenclature

A	constant defined by DM^b at zero concentration
A'	constant defined by $DM^{b'}$ in concentrated solutions
b	FFF channel breadth
b	exponent scaling D to M at infinite dilution
b'	exponent scaling D to M in concentrated solutions
c_{inj}	sample concentration before injection
c_{00}	concentration at centre zone at the accumulation wall
c^*	polymer critical concentration
d_h	particle hydrodynamic diameter
D	diffusion coefficient
D_0	diffusion coefficient at infinite dilution
D_{app}	apparent diffusion coefficient
$\mathfrak{K}$	Boltzmann constant
f	friction coefficient
F	force exerted by the field
ℓ	characteristic thickness of solute zone
L	channel length
M	polymer molecular mass
N	number of polymer segments
R_0	radius of spherical particle
t^0	void time
t_r	retention time
T	absolute temperature
U	field-induced velocity
$\dot{V}$	volumetric channel flow rate
$\dot{V}_c$	volumetric cross-flow rate
V_{inj}	volume injected
V^0	void volume
x	channel transverse coordinate
w	channel thickness
z	axial coordinate
Z	downstream distance of the zone

Greek symbols

α	correcting factor in the A′ term of Eq. (9)
η	fluid viscosity
λ	retention parameter
μ	polymer polydispersity index
σ_{inj}	standard deviation in zone spreading due to injected volume
σ_{neq}	standard deviation in zone spreading due to non-equilibrium effects
σ_{poly}	standard deviation in zone spreading due to sample polydispersity
Φ	exponent defined by $b' - b$

References

[1] I.W. Sutherland, Int. Biodeterior. Biodegrad. (1996) 249.
[2] P.A. Gibbs, R.J. Seviour, in: S. Dumitriu (Ed.), Polysaccharides. Structural Diversity and Functional Versatility, Marcel Dekker, New York, 1995.
[3] J.W. Lee, W.G. Yeomans, A.L. Allen, F. Deng, R.A. Gross, D.L. Kaplan, Appl. Environ. Microbiol. 65 (1999) 5265.
[4] J.C. Giddings, Unified Separation Science, Wiley, New York, 1991.
[5] J.C. Giddings, J. Chem. Edu. 50 (1973) 667.
[6] C. Tanford, Physical Chemistry of Macromolecules, Wiley, New York, 1961.

[7] J.C. Giddings, Y.H. Yoon, K.D. Caldwell, M.N. Myers, M.E. Hoving, Sep. Sci. 10 (1975) 447.
[8] M.E. Hoving, G.H. Thompson, J.C. Giddings, Anal. Chem. 42 (1970) 195.
[9] J.C. Giddings, G. Karaiskakis, K.D. Caldwell, Sep. Sci. Technol. 16 (1981) 725.
[10] L.K. Smith, M.N. Myers, J.C. Giddings, Anal. Chem. 49 (1977) 1750.
[11] J.C. Giddings, Dynamics of Chromatography, Marcel Dekker, New York, 1965.
[12] K.D. Caldwell, S.L. Brimhall, Y. Gao, J. Appl. Polym. Sci. 36 (1988) 703.
[13] A. Ohshima, A. Yamagata, T. Sato, A. Teramoto, Macromolecules 32 (1999) 8645.
[14] A.I. Sagidullin, A.M. Muzafarov, M.A. Krykin, A.N. Ozerin, V.D. Skirda, G.M. Ignat'eva, Macromolecules 35 (2002) 9472.
[15] G.D.J. Phillies, Macromolecules 20 (1987) 558.
[16] G.D.J. Phillies, Macromolecules 35 (2002) 7414.
[17] K. Nishinari, K. Kohyama, P.A. Williams, G.O. Phillips, W. Burchard, K. Ogino, Macromolecules 24 (1991) 5590.
[18] G.M. Pavlov, E.V. Korneeva, N.P. Yevlampieva, Int. J. Biol. Macromol. 16 (1994) 318.
[19] M.-A. Benincasa, K.D. Caldwell, J. Chromatogr. A 925 (2001) 159.
[20] M.-A. Benincasa, J.C. Giddings, Anal. Chem. 64 (1992) 790.
[21] W.F. Reed, S. Ghosh, G. Medjahdi, J. François, Macromolecules 24 (1991) 6189.
[22] W-J. Cao, M.N. Myers, P.S. Williams, J.C. Giddings, Int. J. Polym. Anal. Charact. 4 (1998) 407.
[23] T. Kato, T. Katsuki, A. Takahashi, Macromolecules 17 (1984) 1726.
[24] M.-A. Benincasa, C. Delle Fratte, V. Mazzoni, to be submitted.